



Published in final edited form as:

Microcirculation. 2019 July ; 26(5): e12540. doi:10.1111/micc.12540.

Deletion of *Robo4* prevents high fat diet induced adipose artery and systemic metabolic dysfunction

Tam T.T. Phuong¹, Ashley E. Walker^{1,+}, Grant D. Henson^{1,+}, Daniel R. Machin¹, Dean Y. Li^{4,5,6,^}, Anthony J. Donato^{1,2}, Lisa A. Lesniewski^{1,2}

¹University of Utah, Department of Internal medicine, Division of Geriatrics.

²Salt Lake City Veteran's Affair Medical center, Geriatrics research education and Clinic center.

³University of Utah, Department of Nutrition and Integrative Physiology

⁴Department of Medicine, Program in Molecular Medicine, University of Utah, 15 North 2030 East, Salt Lake City, UT 84112, USA

⁵Division of Cardiovascular Medicine Department of Medicine, University of Utah, 30 North 1900 East, Salt Lake City, UT 84112, USA

⁶Department of Human Genetics, University of Utah, 15 North 2030 East, Salt Lake City, UT 84112, USA

Abstract

Objective: Accumulating evidence suggests the vascular endothelium plays a fundamental role in the pathophysiology of obesity by regulating the functional status of white adipose and systemic metabolism. Roundabout guidance 4 (*Robo4*) is expressed specifically in endothelial cells and increases vascular stability and inhibits angiogenesis. We sought to determine the role of *Robo4* in modulating cardio-metabolic function in response to high fat feeding.

Methods: We examined exercise capacity, glucose tolerance, and white adipose tissue artery gene expression, endothelium-dependent dilation and angiogenesis in wild type and *Robo4* knockout mice fed normal chow or a high fat diet (HFD).

Results: We found *Robo4* deletion enhances exercise capacity in normal chow fed mice and HFD markedly increased the expression of *Robo4* ligand *Slit2* in white adipose tissue. Deletion of *Robo4* increased angiogenesis in white adipose tissue and protected against HFD-induced impairments in white adipose artery vasodilation and glucose intolerance.

Corresponding Author: Lisa A Lesniewski, Ph.D., Department of Internal Medicine, Division of Geriatrics, University of Utah, VA Medical Center-SLC, GRECC Building 2, Rm 2D08, 500 Foothill Dr. Salt Lake City, UT 84148, (801)582-1565 ext 2046, Lisa.Lesniewski@utah.edu.

[^]currently employed by Merck

⁺currently at University of Oregon

Author Contributions. A.E.W., and L.A.L. conception and design of research; A.E.W, G.D.H, D.R.M., A.J.D., and L.A.L. performed experiments; D.Y.L provided the animal model, D.R.M. and L.A.L. analyzed data; A.E.W, A.J.D. and L.A.L. interpreted results of experiments; L.A.L. prepared figures; T.P and L.A.L drafted manuscript; All authors edited and approved of the final manuscript.

Disclosures. The University of Utah has filed intellectual property rights concerning ARF6 pathways. The University of Utah has licensed technology to Navigen Inc., a biotechnology company owned in part by the University of Utah Research Foundation. D.Y. Li is a cofounder of and consultant to Navigen Inc. No other conflicts of interest, financial or otherwise, are declared by the author(s).

Conclusions: We demonstrate a novel functional role for Robo4 in endothelial cell function and metabolic homeostasis in white adipose tissue, with Robo4 deletion protecting against endothelial and metabolic dysfunction associated with a HFD. Our findings suggest that Robo4-dependent signaling pathways may be a novel target in anti-obesity therapy.

Keywords

white adipose tissue (WAT); endothelial cell; Roundabout guidance 4 (Robo4); metabolism

Introduction

Obesity Prevalence and Complications.

The incidence of overweight/obesity is approaching 60% among United State adults¹. Obesity is a critical risk factor for metabolic disease and is associated with high rates of morbidity and mortality, with related medical costs reaching at least \$100 billion annually^{2,3}. Visceral white adipose tissue (WAT) increases with obesity and is associated with impairments in systemic insulin sensitivity⁴⁻⁸. The WAT serves as the main lipid storage site in the body and buffers circulating lipids by clearing triglycerides from the blood and by suppressing the release of free fatty acids (FFAs) into the circulation after feeding. However, when the adipocyte is dysfunctional and unable to store additional lipid, this buffering capacity is lost leading to the ectopic storage of excess circulating lipids that contribute to impaired insulin action⁹

Importantly, appropriate adipose tissue blood flow (ATBF) is required to meet local metabolic needs and impacts tissue metabolism by controlling nutrient flux. Inadequate vascular networks¹⁰ and impaired nutrient-induced ATBF responses may contribute to impaired lipid clearance, ectopic lipid accumulation and insulin resistance in obesity⁹.

Critical role of endothelial function in the WAT.

The WAT is a highly vascularized, well perfused organ¹¹. Fasted ATBF exceeds that of resting skeletal muscle and ATBF has the capacity to increase several fold after feeding or in response to prolonged fasting or exercise^{11,12}. During fasting and exercise, the increase in ATBF supplies albumin for the transport of the released FFAs to be utilized as energy; whereas in the fed state, ATBF increases substrate delivery promoting triglyceride clearance. ATBF is regulated by a variety of factors including neural and hormonal mediators as well as local factors such as FFAs, adenosine, prostaglandins, and nitric oxide (NO)^{13,14}. One source of the locally produced NO is the endothelial cells of the WAT vasculature. NO is the primary vasodilator molecule released from the vascular endothelium in response to stimulation by agonists or changes in shear stress^{15,16}, and in addition to modulating vascular tone, NO is also an anti-proliferative, anti-inflammatory, anti-thrombotic, pro-angiogenic molecule that plays a critical role in vascular/tissue homeostasis^{17,18}. Endothelial dysfunction after a HFD or with obesity is characterized by reduced NO and impaired vasodilator capacity and has been described in a number of vascular beds including coronary^{19,20} and WAT arteries²¹. In addition to impairing ATBF, vascular/endothelial dysfunction and reductions in NO in WAT arteries may also impair angiogenesis that is required during tissue expansion during times of nutrient excess²².

Vascular endothelial growth factor (VEGF) signaling upstream of NO is a critical stimulator of angiogenesis in WAT that has been implicated in the maintenance of adequate ATBF responses and the appropriate expansion of the WAT mass¹⁰.

Robo4 and Endothelial Function.

Roundabout guidance (Robo) receptors, first described for their role in axon guidance during neuronal growth^{23,24}, are transmembrane receptors that exist in 4 isoforms (Robo1–4). Among the Robo isoforms, Robo4 is the most relevant to angiogenesis as it is specifically expressed in the endothelium²⁵. Robo4 increases vascular stability and inhibits angiogenesis in response to VEGF stimulation^{26–28}. Activation downstream of Robo4 reduces breast cancer tumor growth and metastasis via increased endothelial cell integrity and inhibition of angiogenesis²⁹. Although there is controversy regarding the natural ligands for Robo4³⁰, the guidance cue, Slit homologue 2 (Slit2), has been demonstrated to bind Robo4 and lead to inhibition of chemoattractant-induced cell migration^{27,28,31} and appears to reduce pathological angiogenesis³². Importantly, deletion of Robo4 results in viable, fertile mice with a grossly normal vascular phenotype, except retinal vascularization in response to a hyperoxic insult is enhanced after Robo4 deletion²⁷.

The actions of Robo4 that occur in response to VEGF stimulation are mediated by ADP-ribosylation factor 6 (ARF6)^{26–28}. ARF6, a GTPase activated downstream of VEGF and inhibited by Robo4, impacts diverse actions of the vascular endothelium, including crosstalk with protein kinase B (Akt)^{33,34} and the Rho GTPase family member Rac^{28,35} that lead to endothelial nitric oxide synthase (eNOS) activation,^{33,35} cell migration/cytoskeletal rearrangements^{36,37}, cell motility^{28,36,38}, and angiogenesis^{27,34}. Importantly, the activation of ARF6 promotes eNOS activity and NO production as well as the angiogenic actions of VEGF signaling and these effects may be modulated by its endogenous inhibitor, Robo4 (Figure 1)^{27,28}

Here, we sought to determine the role of *Robo4* in modulating cardio-metabolic function, the influence of HF feeding on the expression of *Robo4* and its ligand, *slit2*, in the WAT as well as the impact of *Robo4* on WAT artery endothelial function and systemic metabolism in the setting of high fat feeding.

MATERIALS and METHODS

Animals

The *Robo4* knockout mouse strain was obtained from Dr. Dean Li, whose laboratory previously demonstrated that this model have reduced vascular stability and increased pathological angiogenesis in the retina²⁷. All mice were housed in the Salt Lake City VA Medical Center's Animal Facility on a 12:12 light: dark cycle and had *ad libitum* access to food and water. All animal procedures followed to the Guide for the Care and Use of Laboratory Animals (2011, 8th Ed) and were approved by the University of Utah and the Salt Lake City VA Medical Center Animal Care and Use Committee.

Cardiometabolic function

To obtain a broad measure of the impact of *Robo4* deletion on cardiometabolic function, a graded treadmill exercise test (GXT) was performed in normal chow fed mice as described in a previous study with slight modification³⁹. Littermate wildtype (*Robo4*^{+/+}; WT) and *Robo4*^{-/-} (KO) male and female mice were acclimated to the treadmill by running on a 25 degree incline for 10 min at 5 m/min followed by 5 min at 7 m/min and finally 5 min at 10 m/min. Treadmill time to exhaustion was assessed two days later by running at a 25 degree incline for 5 min at 5 m/min and then increasing the speed 1 m/min every 3 min until mice could not be encouraged to continue by a light brush to the tail.

High fat feeding

Mice were fed a normal rodent chow (NC: 16% kcal from fat, 55% carbohydrate, 29% protein, 8640 Harlan Teklad 22/5 Standard Rodent Chow) or high fat diet (41% saturated/total fat, 41% from carbohydrate, 18% protein, Harlan Adjusted Fat diet #TD.96132) for 8–10 weeks prior to testing.

Gene expression

To examine the impact of high fat feeding on *Robo4* and its natural ligand, *Slit2*, gene expression was measured in the gonadal WAT (gWAT) of NC and HF fed *Robo4*^{+/+} mice. WAT RNA was isolated using TRIZOL (Sigma-Aldrich) and was converted to complementary DNA using QuantiTect Rev. Transcription Kit (Qiagen, cat#205314). Gene expression for *Robo4* and *Slit2* were assessed by quantitative Real Time Polymerase Chain Reaction using RT² SYBR Green qPCR Mastermix (Qiagen, cat#330503). 18S rRNA was used as internal control. mRNA expression was calculated as the fold difference in expression of target mRNA to 18S rRNA for each animal ($2^{-(\text{target CT} - 18\text{S CT})}$).

Primers:

Robo4 forward: 5'-GGAGTGACCTTAAGATCTGGCAAC-3'

reverse: 5'-CTAGTAGCAGCAACCAGAGTAG-3'

Slit2 forward: 5'-GGGAACGACAGTTTCATAGGACTC-3'

reverse: 5'-GTAGTTAGAGAGTTCCTTCGGG-3'

Endothelial function

Vasodilation.—To explore the impact of *Robo4* deletion on HFD associated endothelial dysfunction in the WAT, we examined endothelium dependent (EDD) and independent (EID) vasodilation in isolated gWAT resistance arteries and angiogenesis in gWAT explants from NC and HF fed male and female *Robo4*^{+/+} and *Robo4*^{-/-} mice. To do so, mice were euthanized under isoflurane anesthesia by exsanguination via cardiac puncture. gWAT was placed in cold (4°C) physiological salt solution (PSS) and resistance sized arteries (i.e., <300 μm maximal luminal diameter) were dissected and placed in the chamber of a pressure myograph (DMT Inc., Atlanta, GA, USA) containing PSS. Arteries were cannulated onto glass pipettes, pressurized and warmed to 37° C for 1 hr. Arteries were pre-constricted with

2 μM phenylephrine. The contribution of NO to dilation were measured in response to the cumulative addition of insulin (0.01 to 10 nM) in the absence or presence of the NO synthase inhibitor, N^G-nitro-L-arginine methyl ester (L-NAME: 0.1 mmol/L, 30 min) (N=6–12/group). EID was assessed by measuring a response to sodium nitroprusside (SNP: 1×10^{-10} to 1×10^{-4} mol/L)^{40,41}. Changes in lumen diameter were visualized and assessed using Myoview software (DMT).

Angiogenesis.—gWAT was excised and cut in to small pieces (1mm²). The explants of the gWAT (N=6–8/group) were embedded in a collagen matrix and cultured in standard medium supplemented with vascular endothelial growth factor (VEGF: 0.5 mg/ml). Growth medium changes were performed every other day. Five days after explanation, sprouts were assessed by visualizing cultures with phase-contrast on an inverted microscope (Nikon). Six explants per animal were separately embedded and the total sprouts in these six cultures were averaged and used in the analysis.

Metabolic function.

Fasted blood glucose and glucose tolerance tests (GTTs) were used to assess the impact of *Robo4* deletion on HFD associated impairments in metabolic function. Glucose tolerance tests were performed as described previously⁴². Briefly, mice were fasted for 4 hr in the morning prior to the GTT. Fasted blood glucose was assed prior to the administration of glucose intraperitoneally (GTT: 2 mg/kg) in conscious mice. Blood glucose was subsequently measured 15, 30, 45, 60, and 90 min after injection and both the glucose response curve and the calculated area under the curve for glucose (AUC_{glc}) during the GTT were used in the analyses. Blood glucose was measured using a Precision Xceed Pro Glucose Analyzer.

Statistical Analyses

Group differences in the following data were determined by *t*-test, ANOVA or Repeated Measures ANOVA with LSD post hoc testing where appropriate. Significance was determined at $p < 0.05$. Data are presented as the means \pm SEM.

RESULTS

Exercise capacity is increased in *Robo4*^{-/-} mice.

Exercise capacity was assessed in NC fed mice by GXT as a marker of cardio-metabolic function³⁹. Here, we find that both treadmill time to exhaustion (KO:54.4 \pm 0.5 vs. WT:52.2 \pm 0.7 min, $p=0.02$) and distance travelled (KO:701 \pm 32 vs. WT:655 \pm 15 m, $p=0.02$) during the GXT were higher in *Robo4*^{-/-} (KO) compared to *Robo4*^{+/+} (WT) mice (N=7–12/group).

Slit2, but not *Robo4*, gene expression is higher in gWAT from wildtype mice after HFD.

Consumption of HFD increased gene expression for *Slit2* (N=7–8/group, $p=0.01$) in the gWAT compared to NC fed mice (Figure 2). However, HFD was without effect on gWAT gene expression for *Robo4* (N=6–8/group, $p=0.22$) (Figure 2).

Influence of *Robo4* on body and tissue masses and adipocyte area.

There was no effect of *Robo4* deletion on body ($p=0.73$), liver ($p=0.78$), gastrocnemius muscle ($p=0.45$), or gWAT ($p=0.31$) masses ($N=12-16/\text{group}$) in NC mice (Figure 3 A–D), and body mass was higher in both *Robo4*^{+/+} ($p=0.05$) and *Robo4*^{-/-} ($p=0.01$) after HFD compared to matched NC fed mice (Figure 3 A). Although liver mass was higher after HFD in *Robo4*^{+/+} ($p=0.03$), the increase in liver mass in *Robo4*^{-/-} failed to reach significance ($p=0.07$) (Figure 3B). Gastrocnemius muscle mass was not impacted by HFD in either group (Figure 3C). Similar to the changes observed in body mass, gWAT mass increased after HFD in both the *Robo4*^{+/+} ($p<0.01$) and *Robo4*^{-/-} ($p<0.01$) (Figure 3D). Interestingly, the increase in gWAT mass may be associated with different adipose tissue phenotypes as adipocyte area, assessed in hematoxylin and eosin stained sections of the gWAT ($N=4-7/\text{group}$), was higher ($p<0.01$) after HFD in the *Robo4*^{-/-} mice, whereas adipocyte area was not impacted by HFD in gWAT from *Robo4*^{+/+} mice ($P=0.53$) (Figure 3E). Despite no differences in adipocyte counts between NC fed *Robo4*^{+/+} and *Robo4*^{-/-} (186 ± 15 vs. 225 ± 29 adipocytes/field, $p=0.23$) mice, the HFD-associated changes in adipocyte area were associated with a reduction in the total adipocyte number per histological field in the *Robo4*^{-/-} (122 ± 7 adipocytes/field, $p=0.02$) but not *Robo4*^{+/+} (199 ± 24 adipocytes/field, $p=0.63$) mice, such that there were fewer adipocytes per field in the HF fed *Robo4*^{-/-} compared to diet-matched *Robo4*^{+/+} mice ($p=0.03$).

Deletion of *Robo4* protected endothelial cell function in gWAT.

In NC mice, there was no difference in the insulin concentration-response curves ($p=0.92$) or maximal vasodilation ($p=0.93$) to insulin in gWAT arteries from *Robo4*^{+/+} and *Robo4*^{-/-} mice (Figure 4A–B). Inhibition of eNOS by L-NAME reduced maximal vasodilation to insulin in arteries from NC fed *Robo4*^{+/+} ($p<0.01$) and *Robo4*^{-/-} ($p<0.01$) mice (Figure 4B), indicating the NO plays a significant role in dilation in response to insulin in arteries from both *Robo4*^{+/+} and *Robo4*^{-/-} mice. HFD lowered the insulin concentration-response curves in both *Robo4*^{+/+} ($p=0.08$) and *Robo4*^{-/-} ($p=0.17$) mice, but these differences failed to reach significance. However, maximal vasodilation to insulin was lower in *Robo4*^{+/+} ($p=0.04$), but not *Robo4*^{-/-} ($p=0.18$), mice after HFD, suggesting a modest vaso-protective effect of *Robo4* deletion. L-NAME inhibition reduced dilation to insulin in both *Robo4*^{+/+} ($p<0.01$) and *Robo4*^{-/-} ($p<0.01$) mice after HFD, suggesting that although NO may be reduced, it is still a significant contributor to insulin-induced dilation in gWAT arteries of both *Robo4*^{+/+} and *Robo4*^{-/-} mice after HFD. There was no effect of either *Robo4* deletion or HFD on endothelium independent vasodilation to SNP (data not shown).

Angiogenic sprouting was also assessed by quantifying sprout formation from gWAT explants in vitro as previously described^{43,44}. There was no effect of *Robo4* deletion on angiogenic sprouting in gWAT excised from NC fed mice ($p=0.36$) (Figure 4C) and although HFD was without effect on angiogenic sprouting in gWAT from *Robo4*^{+/+} mice ($p=0.27$), sprouting was higher after HFD in *Robo4*^{-/-} mice ($p=0.04$) (Figure 4C).

Deletion of *Robo4*^{-/-} ameliorated HFD-associated glucose intolerance.

To explore the impact of *Robo4* deletion on metabolic homeostasis, fasted (4 hr) blood glucose and glucose tolerance was assessed in male and female *Robo4*^{+/+} and *Robo4*^{-/-}

mice. While *Robo4* deletion did not impact fasted blood glucose in NC fed mice ($p=0.18$) (Figure 5A), fasted blood glucose was higher after HFD in *Robo4^{+/+}* ($p=0.02$), but not *Robo4^{-/-}* ($p=0.11$), compared to NC fed mice (Figure 5A). Similarly, we found that *Robo4* deletion was without effect on time-response curve for blood glucose ($p=0.26$) or the area under the curve (AUC) for glucose ($p=0.30$) during the GTT in NC fed mice. HFD led to increased blood glucose during the time-response curve ($p<0.01$) and an increased area under the curve for glucose during the GTT ($p<0.01$) in the *Robo4^{+/+}* mice. However, *Robo4^{-/-}* mice were protected against the HFD-associated glucose intolerance. Indeed, we found no difference in blood glucose in the time-response curve ($p=0.10$) or the AUC for glucose during the GTT ($p=0.12$) after HFD in the *Robo4^{-/-}* (Figure 5B–C).

DISCUSSION.

To our knowledge this is the first study to examine the role of the endothelial specific signaling molecule, *Robo4*, in adipose artery and metabolic function, and the response to HF feeding. Here, we demonstrated that deletion of *Robo4*, can enhance exercise capacity in NC fed mice and that *Slit2*, a ligand for Robo4 activation, is sensitive to HF feeding. Furthermore, we demonstrated that HFD-associated impairments in endothelial and metabolic function can be prevented by *Robo4* deletion, highlighting the important role of the vascular endothelium, in general, and *Robo4* signaling, in particular, in maintaining systemic homeostasis.

Exercise capacity.

Although the mechanisms underlying the observed enhancement of exercise endurance in *Robo4^{-/-}* mice requires further elucidation, these data suggest that modulating Robo4 expression has a broad impact on cardio-metabolic function. As increased angiogenesis, at least in pathological settings²⁷, has previously been demonstrated in *Robo4* knockout mice, it is tempting to propose that *Robo4* deletion may increase vascular density in tissues like the heart and skeletal muscle. This putative increase in vascularity may allow for increased tissue blood flow during exercise, a possibility that requires further study but may be supported by our observation of enhanced HFD-associated WAT angiogenesis in *Robo4* deleted mice.

Gene expression.

The observed increase in gWAT *Slit2* expression suggests that Robo4 signaling may be impacted by HFD and thus may contribute to the associated adipose and systemic dysfunction. While future studies should elucidate the mechanisms underlying increased *Slit2* expression in the adipose after HFD as well as determine if this increase in *Slit2* is associated with enhanced Robo4 signaling in the setting of HFD, recent studies have described a role for adipose derived Slit2 in metabolic homeostasis. In contrast to our findings demonstrating decreased Robo4 to have beneficial effects on metabolic function, a recent study by Svensson et al., described a beneficial effect of a beige adipose tissue derived *Slit2* fragment on glucose homeostasis and energy expenditure⁴⁵, suggesting that Slit2 may have actions independent of Robo4. Likewise, circulating slit2 secreted from brown adipose tissue is reduced in the setting of human Type 2 Diabetes Mellitus⁴⁶. Here,

although we observed an increase in *Slit2* in the gWAT after HFD in WT mice, we do not know if this increase also occurred in the metabolically protected *Robo4*^{-/-} mice. Thus, understanding the independent and interacting roles of Slit2 and Robo4 in metabolic protection against HFD is an important area for future investigation.

Endothelial function.

Endothelial dysfunction after a HFD has been described in a number of vascular beds including coronary^{19,20} and WAT arteries²¹. Here, we demonstrate that deletion of *Robo4* has a modest effect to prevent HFD-associated impairments in EDD, that occurs through preservation of NO bioavailability. Despite, the rather modest effects on adipose resistance artery vasodilator function, *Robo4* deletion has much more profound effects to increase angiogenic sprouting in the WAT after HF feeding. The WAT is unique in that it maintains significant plasticity in adulthood, with an enormous capacity for growth and regression in response to changes in energy balance⁴⁷. Notably, the plasticity of the WAT requires a significant and coordinated plasticity in its circulation, as angiogenic processes in the WAT vasculature must adapt to fluctuations in adiposity to appropriately alter ATBF in support of endocrine function and lipid utilization/storage¹¹. The endothelium of the WAT vasculature serves as a source of the pro-angiogenic precursors and signaling required for this process^{22,48-51}. Also, it was recently reported that endothelial progenitor cells of capillaries can differentiate to mature white and brown adipocytes suggesting coordination of angiogenesis and adipogenesis during adipose tissue expansion⁵². Although the precise physiological signals that regulate the fate of endothelial progenitor cells are yet to be identified, the findings of Tran et al.⁵² raise an exciting possibility in the control of formation of new adipocytes, expansion of white and brown adipose tissues and induction of browning in the WAT. While, in a quiescent state, factors released from adipose, inflammatory and vascular cells in the WAT maintain a balance between vascular homeostasis and angiogenic processes^{48,53,54}, VEGF signaling, a critical stimulator of angiogenesis in WAT, has been implicated in the maintenance of adequate ATBF responses¹⁰ and the appropriate expansion of the WAT mass⁵⁵.

Intriguingly, although HFD appears to modestly increase angiogenic sprouting in wildtype mice, this effect is exaggerated by *Robo4* deletion and is associated with enlarged adipocytes in the knockout mice. While evidence in the literature would suggest that such an enlargement of gWAT adipocytes would be associated with metabolic dysfunction and tissue inflammation⁵⁶, we find metabolic protection in the *Robo4* knockout mice. Although the mechanisms underlying the protection observed in the HF fed *Robo4*^{-/-} despite this adipocyte enlargement are unclear, the enhanced angiogenic sprouting may be critical. The observed increased angiogenic capacity to VEGF stimulation observed in the present study may contribute to greater storage of lipid in the adipose rather than to an ectopic accumulation of lipids, a possibility supported by the larger adipocytes observed in the HF fed *Robo4* deleted mice. Furthermore, if this increase in angiogenic capacity translates to increase tissue vascular density, increases in tissue blood flow/distribution may prevent the tissue hypoxia that may otherwise occur in the face of enlarged adipocytes¹⁰. These are possibilities requiring further elucidation.

Metabolic function.

Recently, several studies provided direct evidence for a critical role of the endothelium *per se* in determining systemic metabolic homeostasis as well as adipose tissue phenotype. Indeed, inactivation of the insulin receptor (IR) specifically in endothelial cells delays insulin action in peripheral tissues⁵⁷. In addition, inactivation of endothelial IRs also delays peripheral insulin action leading to impaired glucose tolerance⁵⁷. Several studies have also demonstrated that modulating angiogenic genes in the endothelium can have profound effects on adipose tissue phenotype and, consequently, systemic metabolism. For example, activation of VEGF receptor 2 (VEGFR2) signaling by retinoic acid induces WAT browning, a process by which white adipose takes on characteristics of brown adipose tissue such as a shift in gene expression profiles, an increase in mitochondrial and the development of multilocular adipocytes, by inducing brown/beige adipogenesis⁵⁸. Likewise, endothelial specific knockout of VEGFR2 can prevent the beiging of WAT in response to stimulation⁵⁹. Beyond adipose browning, inhibition of angiogenesis by blockage VEGFR2 also limits adipose tissue expansion in a mouse model of diet-induced obesity⁶⁰. While, endothelial VEGFR1 deletion leads to a lower body and adipose mass, reduced circulating lipids and improved glucose and insulin tolerance in response to HFD when compared with wildtype mice⁶¹. Taken together, these studies demonstrate a powerful influence of endothelial function on metabolism and adipose tissue homeostasis and suggest that factors modulating endothelial function may be effective therapeutic targets in the setting of obesity and insulin resistance. Here, we explored the role of *Robo4*, a novel angiogenic signaling molecule, in metabolic and adipose tissue function in the setting of HFD and found that deletion of *Robo4* prevents HFD associated glucose intolerance.

Previous studies supporting endothelial function as a critical determinant of metabolic and adipose tissue function have focused primarily on the role of endothelial VEGF signaling or NO production as modulating factors. Indeed, a previous report in the literature demonstrates a critical role for endothelial insulin receptor substrate-associated NO production in metabolic homeostasis⁶². Our findings provide additional support for the critical role of endothelial function in both systemic metabolic function and adipose tissue homeostasis^{48,51,55,63}. Here, we demonstrate that deletion of *Robo4*, an endothelial-specific angiogenic signaling molecule protects against the metabolic consequences of HF feeding and preserves angiogenic capacity in the WAT, despite providing only a modest protection against impaired NO-mediated dilation in response to HFD.

Perspectives.

Our data provide evidence that *Robo4* deletion enhances exercise endurance and angiogenic capacity of the gWAT and affords protection against HF-associated impairments in EDD and glucose intolerance. These results highlight the critical role of the endothelium, in general and endothelial *Robo4* signaling, in particular, in adipose and metabolic homeostasis. These findings support the potential role of targeting *Robo4*-dependent signaling pathways in anti-obesity therapy.

Acknowledgments

Funding information. This work was supported in part by awards from the National Institute of Aging, R01 AG048366, R01 AG050238 and K02 AG045339, National Center for Complementary and Integrative Health K99 AT010017, and by Merit Review Award 1I01BX002151 from the United States (U.S.) Department of Veterans Affairs Biomedical Laboratory Research and Development Service. The contents do not represent the views of the U.S. Department of Veterans Affairs, the National Institute on Aging or the United States Government.

List of abbreviations:

ARF6	ADP-ribosylation factor 6
ATBF	adipose tissue blood flow
AUC	the area under the curve
EDD	endothelium dependent dilation
eNOS	endothelial nitric oxide synthase
FFAs	free fatty acids
GTT	glucose tolerance test
gWAT	gonadal white adipose tissue
HFD	high fat diet
IR	insulin receptor
NC	normal chow
NO	nitric oxide
PSS	physiological salt solution
Robo	Roundabout guidance
Robo4	roundabout guidance 4
<i>Robo4</i>^{-/-}: KO	<i>Robo4</i> knockout mouse strain
Slit2	Slit homolog 2
VEGF	vascular endothelial growth factor
VEGFR2	VEGF receptor 2
WAT	White adipose tissue

REFERENCES

1. Flegal KM, Carroll MD, Ogden CL, Johnson CL. Prevalence and trends in obesity among US adults, 1999–2000. *Jama*. 2002;288(14):1723–1727. [PubMed: 12365955]
2. Abdelaal M, le Roux CW, Docherty NG. Morbidity and mortality associated with obesity. *Ann Transl Med*. 2017;5(7):161. [PubMed: 28480197]

3. Das SR, Kinsinger LS, Yancy WS Jr., et al. Obesity prevalence among veterans at Veterans Affairs medical facilities. *Am J Prev Med.* 2005;28(3):291–294. [PubMed: 15766618]
4. Carey DG, Jenkins AB, Campbell LV, Freund J, Chisholm DJ. Abdominal fat and insulin resistance in normal and overweight women: Direct measurements reveal a strong relationship in subjects at both low and high risk of NIDDM. *Diabetes.* 1996;45(5):633–638. [PubMed: 8621015]
5. Cefalu WT, Wang ZQ, Werbel S, et al. Contribution of visceral fat mass to the insulin resistance of aging. *Metabolism.* 1995;44(7):954–959. [PubMed: 7616857]
6. Apovian CM, Bigornia S, Mott M, et al. Adipose macrophage infiltration is associated with insulin resistance and vascular endothelial dysfunction in obese subjects. *Arterioscler Thromb Vasc Biol.* 2008;28(9):1654–1659. [PubMed: 18566296]
7. Jang Y, Kim OY, Ryu HJ, et al. Visceral fat accumulation determines postprandial lipemic response, lipid peroxidation, DNA damage, and endothelial dysfunction in nonobese Korean men. *J Lipid Res.* 2003;44(12):2356–2364. [PubMed: 12951360]
8. Lee CC, Glickman SG, Dengel DR, Brown MD, Supiano MA. Abdominal adiposity assessed by dual energy X-ray absorptiometry provides a sex-independent predictor of insulin sensitivity in older adults. *J Gerontol A Biol Sci Med Sci.* 2005;60(7):872–877. [PubMed: 16079210]
9. Goossens GH. The role of adipose tissue dysfunction in the pathogenesis of obesity-related insulin resistance. *Physiol Behav.* 2008;94(2):206–218. [PubMed: 18037457]
10. Corvera S, Gealekman O. Adipose tissue angiogenesis: impact on obesity and type-2 diabetes. *Biochim Biophys Acta.* 2014;1842(3):463–472. [PubMed: 23770388]
11. Crandall DL, Hausman GJ, Kral JG. A review of the microcirculation of adipose tissue: anatomic, metabolic, and angiogenic perspectives. *Microcirculation.* 1997;4(2):211–232. [PubMed: 9219215]
12. Bulow J, Madsen J. Human adipose tissue blood flow during prolonged exercise II. *Pflugers Arch.* 1978;376(1):41–45. [PubMed: 568240]
13. Ardilouze JL, Fielding BA, Currie JM, Frayn KN, Karpe F. Nitric oxide and beta-adrenergic stimulation are major regulators of preprandial and postprandial subcutaneous adipose tissue blood flow in humans. *Circulation.* 2004;109(1):47–52. [PubMed: 14662716]
14. Frayn KN, Karpe F, Fielding BA, Macdonald IA, Coppack SW. Integrative physiology of human adipose tissue. *Int J Obes Relat Metab Disord.* 2003;27(8):875–888. [PubMed: 12861227]
15. Smits P, Williams SB, Lipson DE, Banitt P, Rongen GA, Creager MA. Endothelial release of nitric oxide contributes to the vasodilator effect of adenosine in humans. *Circulation.* 1995;92(8):2135–2141. [PubMed: 7554193]
16. Kanai AJ, Strauss HC, Truskey GA, Crews AL, Grunfeld S, Malinski T. Shear stress induces ATP-independent transient nitric oxide release from vascular endothelial cells, measured directly with a porphyrinic microsensor. *Circ Res.* 1995;77(2):284–293. [PubMed: 7614715]
17. Ongini E, Impagnatiello F, Bonazzi A, et al. Nitric oxide (NO)-releasing statin derivatives, a class of drugs showing enhanced antiproliferative and antiinflammatory properties. *Proc Natl Acad Sci U S A.* 2004;101(22):8497–8502. [PubMed: 15173604]
18. Isenberg JS, Martin-Manso G, Maxhimer JB, Roberts DD. Regulation of nitric oxide signalling by thrombospondin 1: implications for anti-angiogenic therapies. *Nat Rev Cancer.* 2009;9(3):182–194. [PubMed: 19194382]
19. Kang LS, Reyes RA, Muller-Delp JM. Aging impairs flow-induced dilation in coronary arterioles: role of NO and H₂O₂. *Am J Physiol Heart Circ Physiol.* 2009;297(3):H1087–1095. [PubMed: 19617414]
20. Erdei N, Toth A, Pasztor ET, et al. High-fat diet-induced reduction in nitric oxide-dependent arteriolar dilation in rats: role of xanthine oxidase-derived superoxide anion. *Am J Physiol Heart Circ Physiol.* 2006;291(5):H2107–2115. [PubMed: 16798827]
21. Donato AJ, Henson GD, Morgan RG, Enz RA, Walker AE, Lesniewski LA. TNF-alpha impairs endothelial function in adipose tissue resistance arteries of mice with diet-induced obesity. *Am J Physiol Heart Circ Physiol.* 2012;303(6):H672–679. [PubMed: 22821989]
22. Rupnick MA, Panigrahy D, Zhang CY, et al. Adipose tissue mass can be regulated through the vasculature. *Proc Natl Acad Sci U S A.* 2002;99(16):10730–10735. [PubMed: 12149466]

23. Brose K, Bland KS, Wang KH, et al. Slit proteins bind Robo receptors and have an evolutionarily conserved role in repulsive axon guidance. *Cell*. 1999;96(6):795–806. [PubMed: 10102268]
24. Kidd T, Brose K, Mitchell KJ, et al. Roundabout controls axon crossing of the CNS midline and defines a novel subfamily of evolutionarily conserved guidance receptors. *Cell*. 1998;92(2):205–215. [PubMed: 9458045]
25. Okada Y, Funahashi N, Tanaka T, et al. Endothelial cell-specific expression of roundabout 4 is regulated by differential DNA methylation of the proximal promoter. *Arterioscler Thromb Vasc Biol*. 2014;34(7):1531–1538. [PubMed: 24855053]
26. London NR, Zhu W, Bozza FA, et al. Targeting Robo4-dependent Slit signaling to survive the cytokine storm in sepsis and influenza. *Sci Transl Med*. 2010;2(23):23ra19.
27. Jones CA, London NR, Chen H, et al. Robo4 stabilizes the vascular network by inhibiting pathologic angiogenesis and endothelial hyperpermeability. *Nat Med*. 2008;14(4):448–453. [PubMed: 18345009]
28. Jones CA, Nishiya N, London NR, et al. Slit2-Robo4 signalling promotes vascular stability by blocking Arf6 activity. *Nat Cell Biol*. 2009;11(11):1325–1331. [PubMed: 19855388]
29. Zhao H, Ahirwar DK, Oghumu S, et al. Endothelial Robo4 suppresses breast cancer growth and metastasis through regulation of tumor angiogenesis. *Mol Oncol*. 2016;10(2):272–281. [PubMed: 26778715]
30. Yadav SS, Narayan G. Role of ROBO4 signalling in developmental and pathological angiogenesis. *Biomed Res Int*. 2014;2014:683025.
31. Park KW, Morrison CM, Sorensen LK, et al. Robo4 is a vascular-specific receptor that inhibits endothelial migration. *Dev Biol*. 2003;261(1):251–267. [PubMed: 12941633]
32. Romano E, Manetti M, Rosa I, et al. Slit2/Robo4 axis may contribute to endothelial cell dysfunction and angiogenesis disturbance in systemic sclerosis. *Ann Rheum Dis*. 2018.
33. Eriksson A, Cao R, Roy J, et al. Small GTP-binding protein Rac is an essential mediator of vascular endothelial growth factor-induced endothelial fenestrations and vascular permeability. *Circulation*. 2003;107(11):1532–1538. [PubMed: 12654612]
34. Lee MJ, Thangada S, Paik JH, et al. Akt-mediated phosphorylation of the G protein-coupled receptor EDG-1 is required for endothelial cell chemotaxis. *Mol Cell*. 2001;8(3):693–704. [PubMed: 11583630]
35. Daher Z, Boulay PL, Desjardins F, Gratton JP, Claing A. Vascular endothelial growth factor receptor-2 activates ADP-ribosylation factor 1 to promote endothelial nitric-oxide synthase activation and nitric oxide release from endothelial cells. *J Biol Chem*. 2010;285(32):24591–24599. [PubMed: 20529868]
36. Burridge K, Wennerberg K. Rho and Rac take center stage. *Cell*. 2004;116(2):167–179. [PubMed: 14744429]
37. Tushir JS, D'Souza-Schorey C. ARF6-dependent activation of ERK and Rac1 modulates epithelial tubule development. *EMBO J*. 2007;26(7):1806–1819. [PubMed: 17363898]
38. Cotton M, Claing A. G protein-coupled receptors stimulation and the control of cell migration. *Cell Signal*. 2009;21(7):1045–1053. [PubMed: 19249352]
39. Petrosino JM, Heiss VJ, Maurya SK, et al. Graded Maximal Exercise Testing to Assess Mouse Cardio-Metabolic Phenotypes. *PLoS One*. 2016;11(2):e0148010.
40. Durrant JR, Seals DR, Connell ML, et al. Voluntary wheel running restores endothelial function in conduit arteries of old mice: direct evidence for reduced oxidative stress, increased superoxide dismutase activity and down-regulation of NADPH oxidase. *J Physiol*. 2009;587(Pt 13):3271–3285. [PubMed: 19417091]
41. Lesniewski LA, Connell ML, Durrant JR, et al. B6D2F1 Mice are a suitable model of oxidative stress-mediated impaired endothelium-dependent dilation with aging. *J Gerontol A Biol Sci Med Sci*. 2009;64(1):9–20. [PubMed: 19211548]
42. Lesniewski LA, Seals DR, Walker AE, et al. Dietary rapamycin supplementation reverses age-related vascular dysfunction and oxidative stress, while modulating nutrient-sensing, cell cycle, and senescence pathways. *Aging Cell*. 2017;16(1):17–26. [PubMed: 27660040]

43. Gealekman O, Guseva N, Hartigan C, et al. Depot-specific differences and insufficient subcutaneous adipose tissue angiogenesis in human obesity. *Circulation*. 2011;123(2):186–194. [PubMed: 21200001]
44. Donato AJ, Henson GD, Hart CR, et al. The impact of ageing on adipose structure, function and vasculature in the B6D2F1 mouse: evidence of significant multisystem dysfunction. *J Physiol*. 2014;592(18):4083–4096. [PubMed: 25038241]
45. Svensson KJ, Long JZ, Jedrychowski MP, et al. A Secreted Slit2 Fragment Regulates Adipose Tissue Thermogenesis and Metabolic Function. *Cell Metab*. 2016;23(3):454–466. [PubMed: 26876562]
46. Kang YE, Choung S, Lee JH, Kim HJ, Ku BJ. The Role of Circulating Slit2, the One of the Newly Batokines, in Human Diabetes Mellitus. *Endocrinol Metab (Seoul)*. 2017;32(3):383–388. [PubMed: 28956369]
47. Rajala MW, Scherer PE. Minireview: The adipocyte--at the crossroads of energy homeostasis, inflammation, and atherosclerosis. *Endocrinology*. 2003;144(9):3765–3773. [PubMed: 12933646]
48. Cao Y Angiogenesis modulates adipogenesis and obesity. *J Clin Invest*. 2007;117(9):2362–2368. [PubMed: 17786229]
49. Cao Y Adipose tissue angiogenesis as a therapeutic target for obesity and metabolic diseases. *Nat Rev Drug Discov*. 2010;9(2):107–115. [PubMed: 20118961]
50. Ledoux S, Queguiner I, Msika S, et al. Angiogenesis associated with visceral and subcutaneous adipose tissue in severe human obesity. *Diabetes*. 2008;57(12):3247–3257. [PubMed: 18835936]
51. Rutkowski JM, Davis KE, Scherer PE. Mechanisms of obesity and related pathologies: the macro- and microcirculation of adipose tissue. *FEBS J*. 2009;276(20):5738–5746. [PubMed: 19754873]
52. Tran KV, Gealekman O, Frontini A, et al. The vascular endothelium of the adipose tissue gives rise to both white and brown fat cells. *Cell Metab*. 2012;15(2):222–229. [PubMed: 22326223]
53. Cao R, Brakenhielm E, Wahlestedt C, Thyberg J, Cao Y. Leptin induces vascular permeability and synergistically stimulates angiogenesis with FGF-2 and VEGF. *Proc Natl Acad Sci U S A*. 2001;98(11):6390–6395. [PubMed: 11344271]
54. Sierra-Honigmann MR, Nath AK, Murakami C, et al. Biological action of leptin as an angiogenic factor. *Science*. 1998;281(5383):1683–1686. [PubMed: 9733517]
55. Sung HK, Doh KO, Son JE, et al. Adipose vascular endothelial growth factor regulates metabolic homeostasis through angiogenesis. *Cell Metab*. 2013;17(1):61–72. [PubMed: 23312284]
56. Wernstedt Asterholm I, Tao C, Morley TS, et al. Adipocyte inflammation is essential for healthy adipose tissue expansion and remodeling. *Cell Metab*. 2014;20(1):103–118. [PubMed: 24930973]
57. Konishi M, Sakaguchi M, Lockhart SM, et al. Endothelial insulin receptors differentially control insulin signaling kinetics in peripheral tissues and brain of mice. *Proc Natl Acad Sci U S A*. 2017;114(40):E8478–E8487. [PubMed: 28923931]
58. Wang B, Fu X, Liang X, et al. Retinoic acid induces white adipose tissue browning by increasing adipose vascularity and inducing beige adipogenesis of PDGFRalpha(+) adipose progenitors. *Cell Discov*. 2017;3:17036. [PubMed: 29021914]
59. Seki T, Hosaka K, Lim S, et al. Endothelial PDGF-CC regulates angiogenesis-dependent thermogenesis in beige fat. *Nat Commun*. 2016;7:12152. [PubMed: 27492130]
60. Tam J, Duda DG, Perentes JY, Quadri RS, Fukumura D, Jain RK. Blockade of VEGFR2 and not VEGFR1 can limit diet-induced fat tissue expansion: role of local versus bone marrow-derived endothelial cells. *PLoS One*. 2009;4(3):e4974.
61. Seki T, Hosaka K, Fischer C, et al. Ablation of endothelial VEGFR1 improves metabolic dysfunction by inducing adipose tissue browning. *J Exp Med*. 2018;215(2):611–626. [PubMed: 29305395]
62. Duncan ER, Crossey PA, Walker S, et al. Effect of endothelium-specific insulin resistance on endothelial function in vivo. *Diabetes*. 2008;57(12):3307–3314. [PubMed: 18835939]
63. Michailidou Z, Turban S, Miller E, et al. Increased angiogenesis protects against adipose hypoxia and fibrosis in metabolic disease-resistant 11beta-hydroxysteroid dehydrogenase type 1 (HSD1)-deficient mice. *J Biol Chem*. 2012;287(6):4188–4197. [PubMed: 22158867]

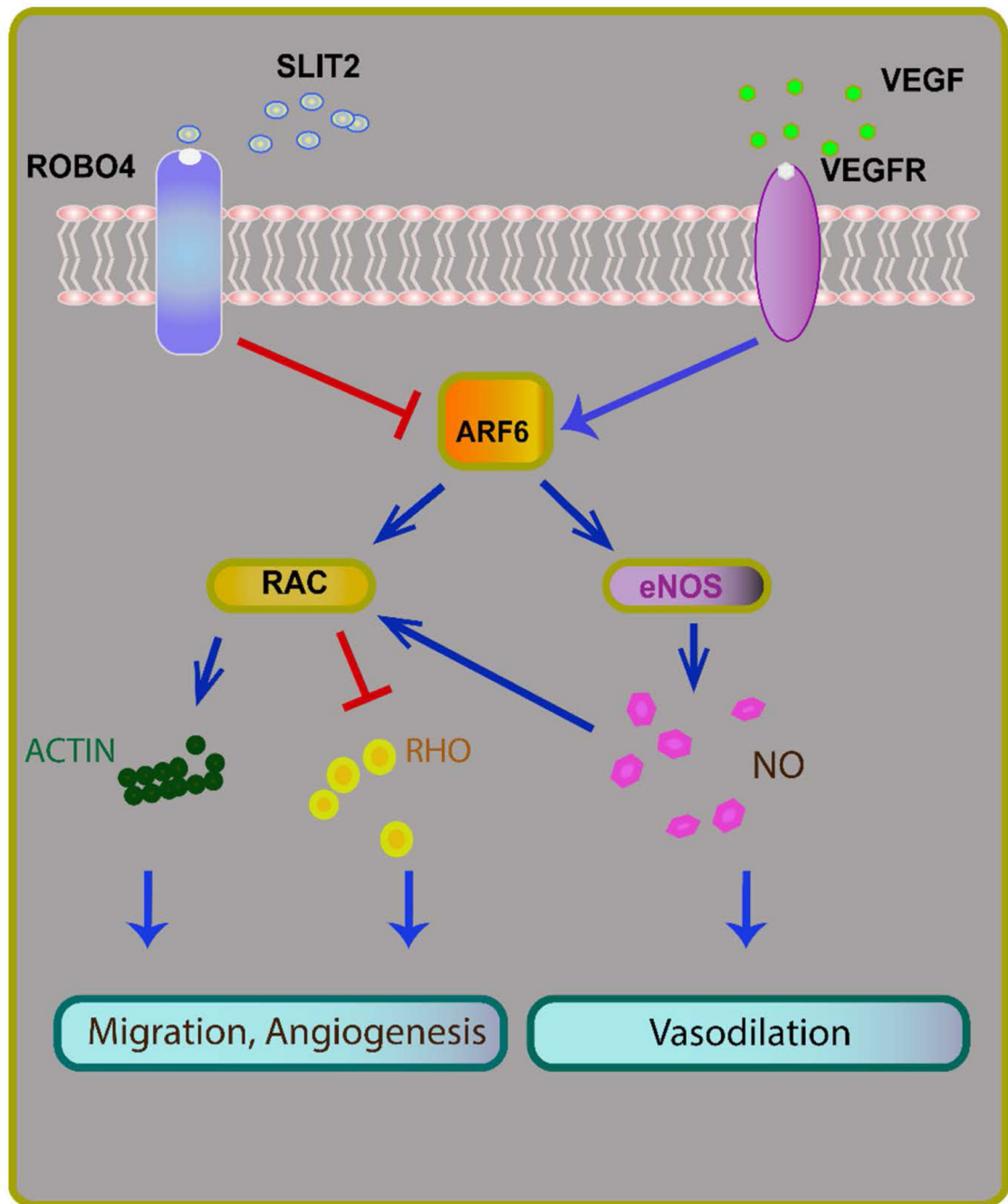


Figure 1. Roundabout guidance receptor 4 (*Robo4*) modulates endothelial function through inhibition of pro-angiogenic vascular endothelial growth factor (VEGF) signaling. When activated by its endogenous ligand slit homolog 2 (Slit2), Robo4, an endothelial specific Robo isoform, inhibits pro-angiogenic VEGF signaling through ADP ribosylation factor 6 (Arf6) and Rac and may reduce nitric oxide mediated vasodilation.

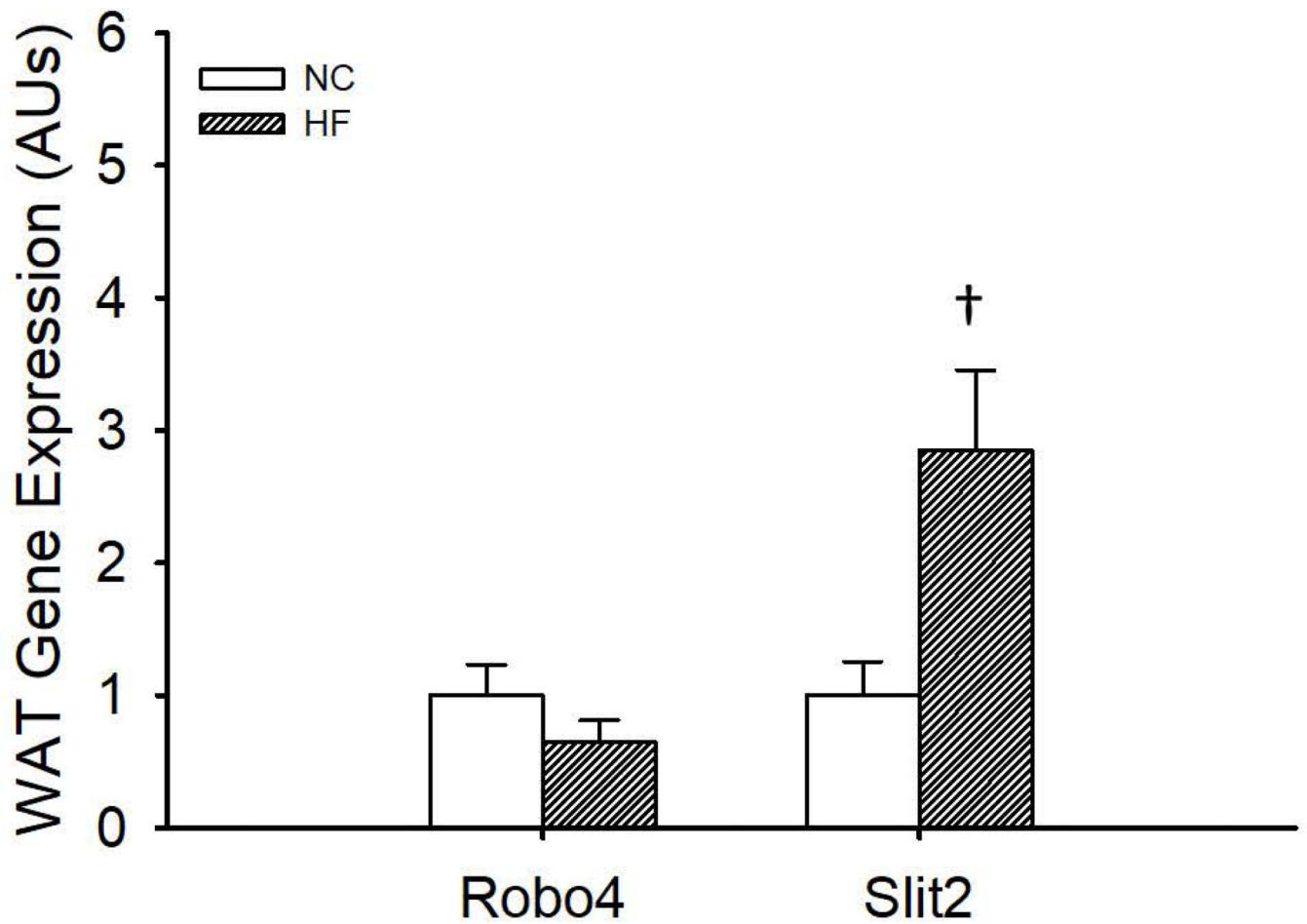


Figure 2.

Gene expression of roundabout receptor 4 (*Robo4*) and Slit homolog 2 (*Slit2*) in the gonadal white adipose tissue (gWAT) of normal chow (NC) and high fat (HF) fed wildtype mice. C57Bl/6 mice (N=6–8/group) were fed NC or HF diet (40% kcal from fat) for 8–10 weeks. gWAT was excised and RNA isolated to assess *Robo4* and *Slit2* gene expression by qPCR. *denotes difference from NC, Data are means \pm SEM, p 0.05

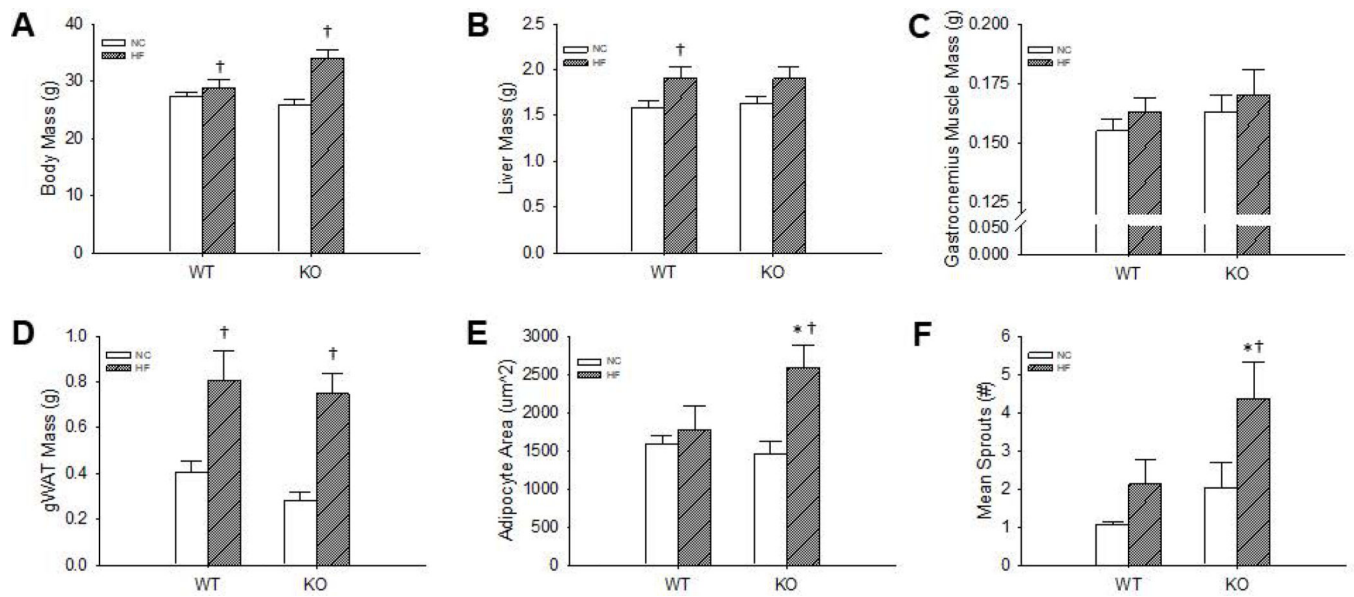


Figure 3.

Body mass (A), liver (B), gastrocnemius muscle (C) and gonadal white adipose tissue (gWAT) (D) tissue masses, and gWAT adipocyte area (E) and angiogenic sprouting (F) in gWAT explants from normal chow (NC) and high fat diet (HF) fed wildtype (WT) and roundabout receptor 4 (*Robo4*) knockout (KO) mice. WT and KO mice were fed either NC or HF (40% fat by kcal) for 8–10 weeks before euthanasia for tissue collection. Adipocyte area was assessed in hematoxylin and eosin stained sections of paraffin embedded gWAT and are presented as the mean area of at least 200 adipocytes/animal. Angiogenic sprouting was assessed in gWAT explants (~1mm³) embedded in matrigel and treated with vascular endothelial growth factor (0.5 mg/ml). Six explants were used per animal and data presented is the mean number of sprouts in these 6 cultures, 5 days after embedding. *denotes difference from NC fed WT, †denotes difference from HF fed of same genotype, Data are means ± SEM, p 0.05

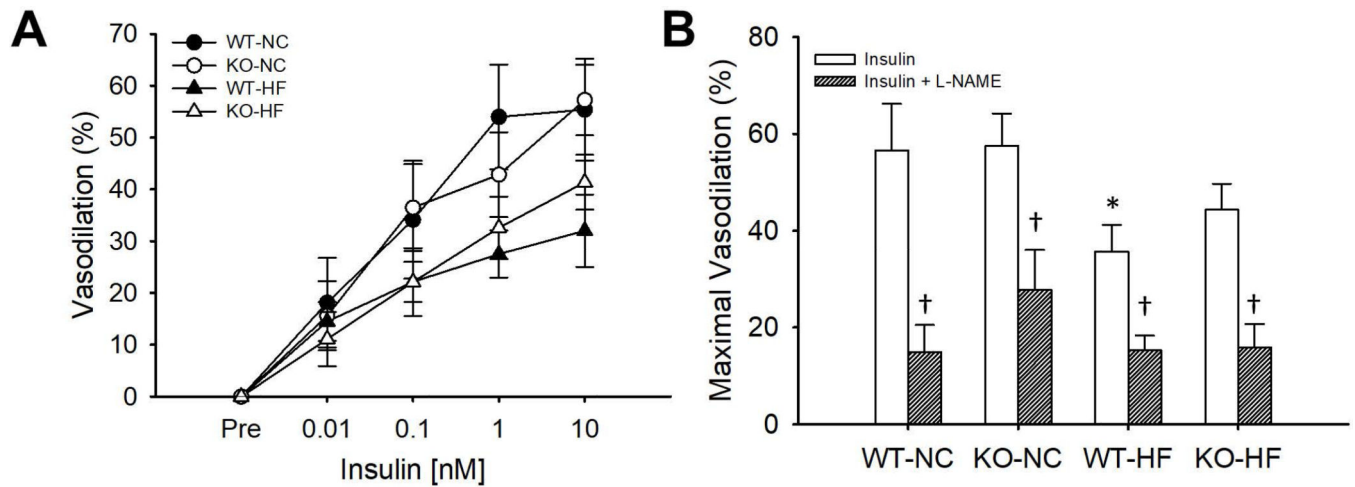


Figure 4.

Concentration-response to insulin in isolated gonadal white adipose tissue (gWAT) feed arteries (**A**) and maximal vasodilation to insulin in the absence or presence of the endothelial nitric oxide synthase inhibitor, L-NAME (**B**) in normal chow (NC) and high fat (HF) fed wildtype (WT) and roundabout receptor 4 (*Robo4*) knockout (KO) mice. WT and KO mice were fed either NC or HF (40% fat by kcal) for 8–10 weeks before euthanasia for tissue collection. gWAT feed arteries were excised, cleared of surrounding tissues and cannulated in the stage of a pressure myograph (DMT Inc.) Arteries were precontracted with phenylephrine and vasodilation was assessed after the cumulative addition of insulin in the absence or presence of L-NAME. *denotes difference from WT-NC, †denotes difference from HF fed of same genotype, Data are means \pm SEM, $p < 0.05$

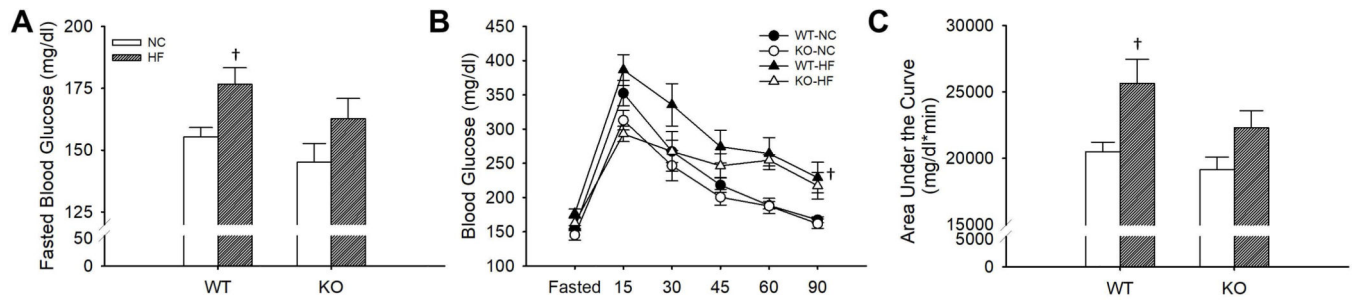


Figure 5.

Fasted blood glucose (A), blood glucose during a glucose tolerance test (GTT) (B) and area under the curve for glucose during the GTT (C) in normal chow (NC) and high fat diet (HF) fed wildtype (WT) and roundabout receptor 4 (*Robo4*) knockout (KO) mice. WT and KO mice were fed either NC or HF (40% fat by kcal) for 8–10 weeks before testing. Mice were fasted for 4 hr and blood was collected via a tail nick. Glucose (2g/kg) was administered intraperitoneally and blood glucose was measured at 15, 30, 45, 60 and 90 after injection. †denotes difference from HF fed of same genotype, Data are means \pm SEM, p 0.05